Observation of phonon modes in epitaxial PbTe films grown by molecular beam epitaxy

Huizhen Wu,[a] Chunfang Cao, Jianxiao Si, Tianning Xu, Hanjie Zhang, and Haifei Wu
Department of Physics, Zhejiang University, Hangzhou, Zhejiang 310027, People's Republic of China

Jing Chen and Wenzhong Shen
Department of Physics, Shanghai Jiao Tong University, Shanghai 200050, People's Republic of China

Ning Dai
National Laboratory for Infrared Physics, Shanghai Institute of Technical Physics, Chinese Academy of Sciences, Shanghai 200083, People's Republic of China

(Received 26 October 2006; accepted 25 January 2007; published online 17 May 2007)

Phonon modes of PbTe films grown by molecular beam epitaxy have been studied by micro-Raman scattering. On the as-grown PbTe surface, strong TeO_2 phonon vibrational modes were detected, which obscured the observation of the longitudinal optical (LO) phonons of PbTe in early conventional Raman scattering experiments. Existence of a TeO_2 layer on the PbTe surface is confirmed by observation with x-ray photoemission spectroscopy. After removal of TeO_2 by chemical etching, the LO phonons for PbTe films were unambiguously observed. Misfit strain accommodated in the epitaxial films makes the lattice distorted from cubic structure, which lowers the crystal symmetry and leads to observation of what would normally be Raman inactive LO phonon modes for PbTe. © *2007 American Institute of Physics*. [DOI: 10.1063/1.2714682]

I. INTRODUCTION

Lead chalcogenide materials (such as PbTe and PbSe) have many interesting characteristics. They have NaCl-type crystal structure and a narrow, direct band gap at the *L* point in the Brillouin zone. Symmetric conduction and valence bands provide good quantum confinement for both electrons and holes in low dimensional structures. The high dielectric constant reduces the negative effects of impurity scattering, making IV-VI materials practical for a variety of applications that require good electrical conductivity.[1–4] Due in part to the absence of a degenerate heavy hole band, nonradiative Auger recombination rate is more than one order of magnitude smaller in comparison with III-V and II-VI materials that have similar narrow band gaps,[5] allowing realization of stimulated emission at relatively low excitation rates. Up to now, the reported highest continuous wave (cw) operation temperature of a midinfrared lead chalcogenide diode laser is 223 K.[6] Limitation in maximum laser operation temperature has been attributed to the low thermal conductivity of IV-VI semiconductor materials; so knowledge of lattice vibrational modes is important for developing potential solutions for increasing operating temperatures. However, the vibrational properties of this material system have not been fully studied because with its NaCl-type crystal structure, where all the atoms at the center of the symmetry (O_h^5), all $q \approx 0$ vibrational modes are Raman inactive.[7] The difficulty in observation of the first- and second-order Raman peaks on the lead chalcogenides was reported by several groups.[8–10] In spite of this restriction, it may be possible to observe Raman scattering since actual synthesized materials are often not of perfect crystalline structure, especially for heteroepitaxial thin films. Any deviation from a perfect crystal, such as nonstoichiometry, deformation, dislocations, or extrinsic doping, could cause vibrational modes to be Raman active. In fact, longitudinal optical (LO) phonon modes in PbSe thin films grown on BaF_2 (111) substrates and in mineral PbS (galena) have already been detected using conventional Raman scattering measurements.[11,12] Raman inactive LO phonons of PbTe were first observed by inelastic neutron scattering of PbTe *bulk crystal* by Cochran *et al.* (114 cm^{-1}).[13] The second observation of LO phonons of PbTe (119 cm^{-1}) was reported by Brillson and Burstein,[8] in which high electric fields of 10^5 V/cm (electric-field-induced scattering) were applied to PbTe bulk crystals. Applying an electric field to a PbTe bulk crystal bends the energy bands and modifies the Raman scattering selection rules by lowering the symmetry of the crystal. Obviously, a difference of the LO frequency between the two observations exists. To the best of our knowledge, direct observation of LO phonons for epitaxial PbTe films has not been reported.

The objectives of this study are to observe the LO phonon mode for epitaxial PbTe and search for the underlying mechanisms that determine its properties. PbTe crystalline films were grown by molecular beam epitaxy (MBE) on BaF_2 (111) substrates and its phonon modes studied by micro-Raman scattering spectroscopy. X-ray photoemission spectroscopy (XPS) was also used to observe the existence of TeO_2 layer on PbTe surface. After removal of TeO_2, the LO phonons for PbTe films were unambiguously observed.

[a]Author to whom correspondence should be addressed; electronic mail: hzwu@zju.edu.cn

II. EXPERIMENT

The PbTe films used in this study were grown on freshly cleaved BaF_2 (111) substrates by MBE. The growth rate of PbTe was 1 μm/h per hour and the final film thickness was about 2 μm. Growth details are described in a previous publication.[14] Atomic force microscopy (AFM) and high-resolution x-ray diffraction (HRXRD) measurements have demonstrated the good crystalline quality of the epitaxial PbTe thin films, i.e., atomically smooth surface with root mean square roughness smaller than 0.5 nm and narrow full width at half maximum of XRD (FWHM $<$100 arc sec). For the measurements of the Raman spectra, an Ar^+ laser (λ =514.5 nm) with a cw output of about 10 mW was used. The laser beam was focused to a spot size of about 1 μm in diameter. A Jobin Yvon LabRAM HR 800 monochromotor and an Ander DU420 classic charge-coupled device (CCD) detector were used. The measured spectral range is from 50 to 500 cm^{-1} with spectral resolution higher than 1 cm^{-1}. A notch filter was used to eliminate the Rayleigh scattering light, which has a low wave number cutoff to $\sim$50 cm^{-1}. All the measurements of Raman spectra were carried out in a backscattering geometry at room temperature. Depth-profiled scans by changing the focus depth (FD) of pumping laser were performed to distinguish the vibrational origins of the observed phonon modes. The depth resolution of the FD scans is better than 0.5 μm. The FD of the pumping laser spot changed from down-surface 3 μm (−3 μm) to up-surface 3 μm (+3 μm) with an interval of 1 μm, and seven spectra were scanned subsequently for each sample. Peak positions and integrated intensities were determined by fitting single Lorentzian curves to the measured data.

To understand whether the existence of tellurium oxide on surface obscures the LO phonons of PbTe, x-ray photoemission spectroscopy was used to characterize surface chemistry. The XPS measurements were performed in a multifunctional ultrahigh-vacuum (UHV) varied temperature scanning probe microscope (VT-SPM) system (Omicron) with a background pressure better than 1×10^{-10} Torr. The system is equipped with an electron-bombardment sample heater, an argon-ion sputter gun, and an x-ray photoemission spectrometer. After confirming the existence of tellurium oxide on the PbTe surface by XPS, the samples were chemically etched to remove the oxide layer on the PbTe surface. The etchant consisted of KOH, H_2O_2, $C_3H_8O_3$, and H_2O with ratios of 20 g:1 ml:2 ml:20 ml. As soon as the PbTe samples were etched to about a 100 nm depth, the sample was characterized again with the Raman spectroscopy measurement system.

III. RESULTS AND DISCUSSION

A. Observation of phonon scattering of TeO_2 formed on the surface of the PbTe film

Figure 1 shows the Raman spectra of a PbTe film grown on BaF_2 (111) with different FD scans. Phonon modes at 87, 143, 183, 243, and 286 cm^{-1} can be clearly resolved in all spectra. Frequency shift with the change of FD is not seen, while their intensities change significantly. When FD varied

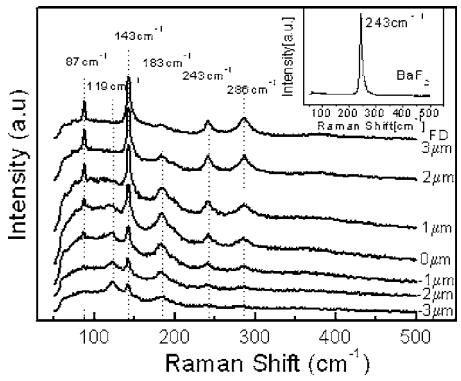

FIG. 1. Raman spectra at seven different focus depths for the as-grown PbTe film on a BaF_2(111) substrate. The inset shows the Raman spectrum of a bare BaF_2 substrate.

from 3 to −3 μm, the integrated peak intensities of the peaks at 87, 143, and 286 cm^{-1} decreased by about ten times.

The mode at 143 cm^{-1} shown in Fig. 1 was already observed in conventional Raman scattering experiments on PbTe bulk crystals (*unstrained*) and was assigned to the vibrational mode of a thin TeO_2 layer formed on PbTe surface.[15–17] It can be seen that the mode at 87 cm^{-1} behaves the same as the mode at 143 cm^{-1}, i.e., as FD goes down, the intensity decreases quickly while the peak position remains unchanged. The mode at 87 cm^{-1} is attributed to the transverse optical (TO) phonon mode of TeO_2, which is formed on the PbTe surface. The mode at 286 cm^{-1} is attributed to the first overtone of the TeO_2 LO mode at 143 cm^{-1}, since its wave number is exactly twice of that of the 143 cm^{-1} mode and intensity variation versus FD is also the same.

The mode at 243 cm^{-1} arises from the BaF_2 substrate, which is verified by the measurement of a bare BaF_2 substrate, as shown in the inset presenting a single narrow Raman peak at 243 cm^{-1} in the whole spectral range from 50 to 500 cm^{-1}. The assignment of this peak is in agreement with the observation reported early in Ref. 11

It is interesting to notice the variation of the phonon mode at 119 cm^{-1} with FD that is shown in Fig. 1. This mode does not show up until FD goes down to 0 μm. The peak intensity increases and its position shifts towards higher frequency with decreasing FD. The intensity versus FD behavior for the mode at 119 cm^{-1} is just the opposite to that of the 87 cm^{-1}, and 143 cm^{-1} modes that originate from the TeO_2 surface layer. In order to confirm the existence of the TeO_2 thin layer on PbTe, we further performed surface characterization of the PbTe sample by using XPS.

B. Observation of tellurium oxide on PbTe surface by XPS

XPS surface characterizations for the as-grown PbTe films confirmed the existence of tellurium oxide on the surface of the epitaxial PbTe film. The XPS spectra of the Te 3*d* peaks of the epitaxial PbTe film are shown in Fig. 2. In the XPS spectrum of the as-grown PbTe sample, two weak peaks centered at 575.83 and 587.10 eV are seen in addition to the two strong peaks at 571.54 and 581.88 eV. The two strong peaks are associated with Te 3*d* states, and the two weak

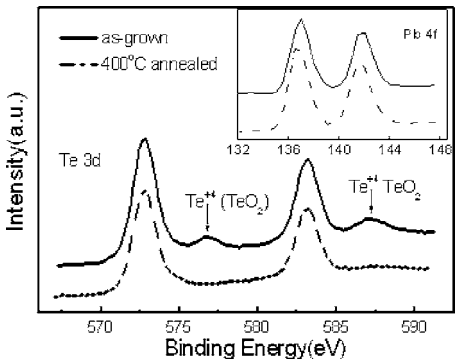

FIG. 2. (a) The measured XPS spectra in the vicinity of the Te 3*d* peaks for the as-grown and 400 °C annealed PbTe film surface.

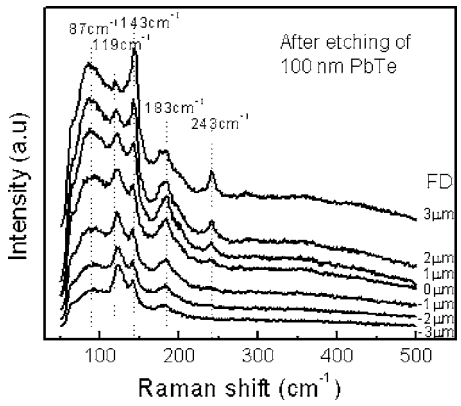

FIG. 3. Raman spectra at seven different focus depths for the etched PbTe film. The enhancement of the LO phonon of PbTe (119 cm^{-1}) and suppression of the LO phonon of TeO_2 surface layer (143 cm^{-1}) were observed.

peaks are attributed to TeO_2 (Te^{4+}) on the surface of PbTe. This assignment is in good agreement with the data of Gran *et al.*[18] To remove the TeO_2 layer on PbTe surface, the sample was thermally annealed in the ultrahigh vacuum XPS chamber. A subsequent XPS measurements on the surface of the PbTe sample were performed after annealing through a temperature ramp from 100 to 400 °C. The measured Te 3*d* peaks are also plotted in Fig. 2. The two weak peaks at 575.83 and 587.10 eV vanish completely after the annealing step. These results are consistent with the thermal desorption of TeO_2 or the decomposition of TeO_2 and evaporation of oxygen. The comparison of the XPS measurements of the asgrown with the 400 °C annealed PbTe films indicates the existence of TeO_2 on the as-grown PbTe surface, which confirms the interpretation of the Raman scattering spectra. Compared with other lead chalcogenides, such as PbS and PbSe, the PbTe surface seems to be more prone to form a TeO_2 surface layer. This phenomenon can be attributed to tellurium (Te) having a more metallic character than sulfur (S) or selenium (Se). Strong Raman scattering by the TeO_2 thin surface layer prevented the observation of peaks associated with scattering by PbTe LO phonons. As shown in the inset of Fig. 2, which plots the portion of the XPS spectrum showing the 4*f* lines of Pb, there are no peaks consistent with a chemical shift associated with PbO. Therefore, a surface oxidation composed of PbO can be excluded.[19]

C. Removal of TeO_2 and unambiguous observation of LO phonon of PbTe

The observation of TeO_2 phonon modes on the surface of the as-grown PbTe film by depth-profiled Raman scattering (Fig. 1) and TeO_2 peaks in the XPS spectrum (Fig. 2) and the difficulty in detecting the LO phonons of epitaxial PbTe films by earlier conventional Raman scattering experiments suggest that PbTe is covered by a TeO_2 oxidation layer. To verify this hypothesis, we proceeded with chemical etching of the as-grown PbTe film to remove the TeO_2 layer. As soon as the etching process was completed, the sample was measured again with the Raman scattering system to obtain FD scans. Figure 3 shows seven Raman spectra with different FDs for the etched PbTe sample. It is interesting to note that the mode at 119 cm^{-1} can be clearly seen in all seven FD scans with enhanced peak intensities in comparison with the as-grown sample shown in Fig. 1, while the intensities of the TeO_2 LO and TO modes (143 and 87 cm^{-1}) were significantly suppressed. The vibrational mode at 119 cm^{-1} is assigned to the LO phonon of the epitaxial PbTe films.

Similar to other narrow gap semiconductors, unintentionally doped PbTe often displays a relatively high electron concentration ($\sim 10^{17}/cm^3$) and coupled plasmon-phonon modes are observed by Raman scattering. The 183 cm^{-1} mode in the Raman spectra shown in both Figs. 1 and 3 is the coupled plasmon-phonon mode of PbTe. The theoretical approach for this mode includes the frequencies of LO and TO phonons (ω_{LO} and ω_{TO}):[20]

$$\omega_{\pm}^2 = \frac{1}{2}(\omega_{LO}^2 + \omega_p^2) \pm \frac{1}{2}[(\omega_{LO}^2 - \omega_p^2)^2 + 16C^2\omega_{LO}\omega_P]^{1/2}, \tag{1}$$

where

$$C = \frac{1}{2}[\omega_{LO}\omega_P(1 - \omega_{TO}^2/\omega_{LO}^2)]^{1/2},$$

$$\omega_p^2 = ne^2/m^*\varepsilon_s.$$

ω_p is the plasma frequency, e the free electron mass, n the carrier concentration, m^* the effective mass, and ε_s the static dielectric constant of PbTe. The TO phonon of PbTe is not observed here due to the response cutoff (50 cm^{-1}) of the notch filter in our Raman system. However, the frequency for the TO phonon mode of PbTe bulk crystal is available in Ref. 13 at 32 cm^{-1}. The samples used here have an electron concentration of $\sim 1\times 10^{17}/cm^3$ as determined by Hall effect measurements. The parameters used in the calculation are $m^*=0.058$, and $\varepsilon_s=380$.[21] Using Eq. (1), we obtain $\omega_+ = 176$ cm^{-1}, which is in agreement with the observed 183 cm^{-1} peak in the Raman spectra.

Figure 4(a) plots the frequency shift of the observed 119 and 143 cm^{-1} phonon modes. As FD goes down from +3 to −3 μm, the PbTe LO phonon mode (119 cm^{-1}) shifts from 119 to 124 cm^{-1}. In contrast, the TeO_2 LO phonon mode (143 cm^{-1}) is almost independent of FD because the TeO_2 surface layer is very thin (~5 nm). The 5 cm^{-1} Raman shift for the PbTe LO mode results from the residual of lattice misfit strain accommodated in the PbTe layer. It is

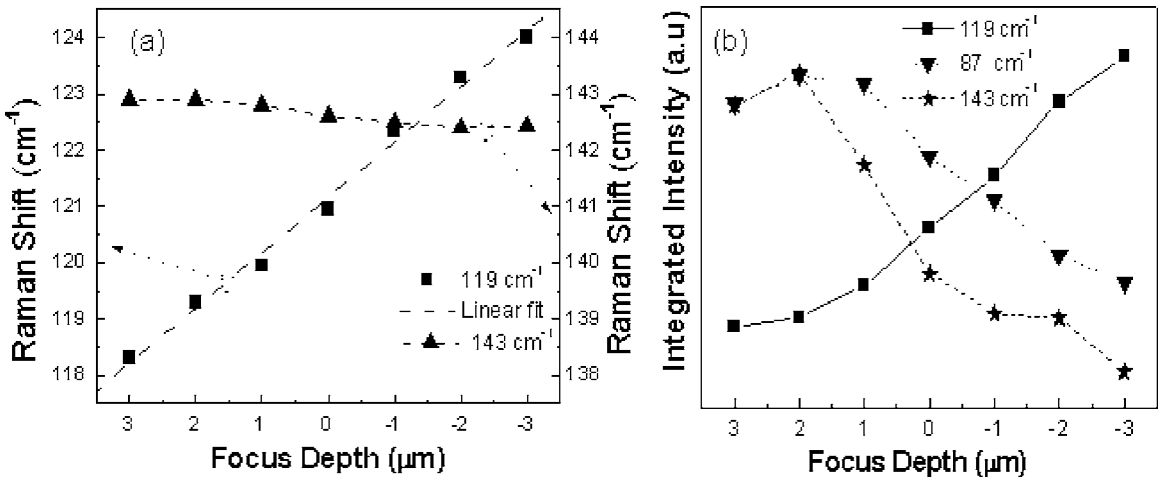

FIG. 4. (a) Peak position vs FD for the 143 and 119 cm^{-1} modes; (b) peak intensity versus FD for the 143, 87, and 119 cm^{-1} modes.

known that both PbTe and the BaF_2 substrate are of cubic crystal structure, but the lattice constant of PbTe (0.644 nm) is larger than that of BaF_2 (0.620 nm). Therefore, the epitaxial growth of PbTe on (111) BaF_2 surfaces will produce a biaxial compression of the PbTe unit cell along the x and y directions parallel to the growth surface. The nonzero components of the strain tensor are $\varepsilon_{xx}=\varepsilon_{yy}=\varepsilon=(a_{\parallel}-a_{BaF_2})/a_{BaF_2}$ and $\varepsilon_{zz}=2S_{12}/(S_{11}+S_{12})\varepsilon$. Here, S_{11} and S_{12} are elastic compliance constants. In this material system, the PbTe thin film is compressively strained and ε is +4.1%. The compressive stress makes the PbTe lattice distorted from a cubic structure, leading to the change in lattice vibrational frequency. With the increase of the epilayer thickness, however, the misfit strain gradually relaxes and the lattice vibrational frequency approaches the value for unstrained PbTe (119 cm^{-1}). The Raman scattering intensity for the PbTe LO phonon mode also decreases as the frequency approaches 119 cm^{-1}, indicating a trend towards the unstrained symmetrical state of PbTe where the LO phonon mode is Raman inactive.

By fitting the experimental data of the Raman peak shifts shown in Fig. 4(a), the PbTe LO phonon frequency variation with FD can be described by following formula:

$$\omega = 121.3 - 0.98Z \quad (-3 \leqslant Z \leqslant 3). \tag{2}$$

The linear relationship between the Raman peak frequency and the FD indicates a linear reduction of compressive strain near the top surface of the PbTe thin films, as compared with the strain value representative of the regions of the sample closer to the interface with the BaF_2 substrate. In the epitaxy of PbTe on lattice mismatched BaF_2, as film thickness increases, the compressive strain is relaxed gradually.

The observed linear variation of the LO phonon frequency of PbTe with FD indicating the linear strain relaxation with the film thickness is in agreement with the theoretical approach of Cerdeira *et al.*:[22]

$$\omega = \omega_{LO} + 2\Delta\Omega_H - \frac{2}{3}\Delta\Omega, \tag{3}$$

where

$$\Delta\Omega_H = \frac{p+2q}{6\omega_{LO}^2}\left(\frac{S_{11}+2S_{12}}{S_{11}+S_{12}}\right)\omega_{LO}\varepsilon$$

is the shift due to the hydrostatic component of the stress and

$$\Delta\Omega = \frac{p-q}{2\omega_{LO}^2}\left(\frac{S_{11}-S_{12}}{S_{11}+S_{12}}\right)\omega_{LO}\varepsilon$$

is the shift due to the uniaxial component of the stress.

Here, ω_{LO} is the LO frequency of undisturbed bulk PbTe crystal; p and q are phenomenological coefficients describing the changes in the "spring constant" of the optical phonon with strain. Therefore, the relation of frequency of LO phonon versus strain can be written as a linear equation:

$$\omega = 119 + A\omega_{LO}\varepsilon, \tag{4}$$

where

$$A = \frac{pS_{12}+q(S_{11}+S_{12})}{\omega_{LO}^2(S_{11}+S_{12})}.$$

Equation (4) predicts linear blueshifts in ω for positive ε, which is in qualitative agreement with our measurement of linear Raman peak shifts with FD. Further, the constant A can be determined experimentally by application of hydrostatic pressure to PbTe samples in the measurements of Raman scattering spectra.

Figure 4(b) plots the FD dependence of the integrated peak intensities of the 143, 87, and 119 cm^{-1} vibrational modes. The data for the 143 and 87 cm^{-1} modes of TeO_2 are taken from the as-grown PbTe sample, while the data for the 119 cm^{-1} mode of PbTe are taken from the etched PbTe sample. It is clearly seen that as FD goes down from +3 to −3 μm, the intensity of the 119 cm^{-1} mode (LO of PbTe) *increases*, while the intensity of the 143 and 87 cm^{-1} modes of TeO_2 *decreases*. The Raman peak shift and intensity variation with FD show that 119 cm^{-1} mode has different origin from the 143 and 87 cm^{-1} modes and the vibrational mode at 119 cm^{-1} originated from the LO phonons in the epitaxial PbTe films.

As seen in Fig. 3, after chemical etching of the epitaxial PbTe film, the PbTe LO mode (119 cm^{-1}) is enhanced while

TABLE I. The summary of each Raman peak and its assignment.

Raman peak (cm^{-1})	87	119	143	183	243	286
Assignment	TO (TeO_2)	LO (PbTe)	LO (TeO_2)	CPPM[a] (PbTe)	LO (BaF_2)	2LO (TeO_2)

[a]CPPM-the coupled plasma-phonon mode.

the TeO_2 LO mode (143 cm^{-1}) is suppressed. However, the TeO_2 LO modes can still be seen. The maintenance of the TeO_2 LO modes in the etched sample indicates reoxidation of the freshly exposed PbTe surface because of its exposure to the atmosphere during the Raman scattering measurements.

The assignments of the vibrational mode at 119 cm^{-1} to the LO phonons of the epitaxial PbTe films and 143 cm^{-1} mode to the LO phonons of TeO_2 surface layer are supported by the following arguments: (1) the clear observation of TeO_2 layer on the as-grown PbTe surface by XPS; (2) the enhancement of the ~119 cm^{-1} mode and the suppression of the TeO_2 modes (87 and 143 cm^{-1}) for the freshly etched PbTe as compared with the Raman spectra of the as-grown PbTe film sample; (3) the obvious difference in the FD dependence of the peak position and intensity of the 119 cm^{-1} mode from the TeO_2 modes at 87 and 143 cm^{-1}; and (4) the assignment of the 119 cm^{-1} mode to the LO phonons of PbTe film being in good agreement with the results observed from strain-free PbTe bulk crystals by surface electric-field-induced Raman scattering (119 cm^{-1}) (Ref. 8) and close to the value of 114 cm^{-1} obtained by inelastic neutron scattering for PbTe bulk crystals.[13] The residual strain in the epitaxial PbTe thin films is responsible for the observation of the PbTe LO phonon. When PbTe was epitaxially grown on lattice mismatched BaF_2 (111) by MBE, the crystal symmetry of the cubic structure was lowered due to the lattice distortion from cubic crystal structure, leading to the activation of the LO Raman mode in epitaxial PbTe films. In summary, the assignments for each Raman peak shown in Figs. 1 and 3 are listed in Table I.

V. CONCLUSION

Epitaxial PbTe thin films were grown by molecular beam epitaxy (MBE) on BaF_2 (111) substrates. In the as-grown PbTe samples, strong TeO_2 phonon vibration modes were detected, which obscured the observation of longitudinal optical phonons for PbTe. XPS characterization confirmed the formation of a TeO_2 layer on the PbTe surface. After removal of the TeO_2 surface layer by chemical etching, the LO phonon for epitaxial PbTe film was unambiguously observed. With FD changing from up- to down-surface 3 μm, the LO phonon peak of PbTe varied from 119 to 124 cm^{-1}, which is attributed to variation of the residual of strain in the PbTe epitaxial films grown on the lattice mismatched BaF_2 (111) substrate. The misfit strain makes the PbTe lattice distorted from a cubic structure that leads to the lowering of crystal symmetry and the Raman activation of epitaxial PbTe films. The observed coupled plasmon-phonon mode is in agreement with theoretical calculation.

ACKNOWLEDGMENTS

The authors would like to thank Professor P. McCann in Oklahoma University for the useful discussion and the correction of the usage of English. This work has been supported by the National Natural Science Foundation of China under Grant Nos. 10434090 and 10125416.

[1] D. V. Talapin and C. B. Murray, Science **310**, 86 (2005).
[2] R. D. Schaller, J. M. Pietryga, S. V. Goupalov, M. A. Petruska, S. A. Ivanov, and V. I. Klimov, Phys. Rev. Lett. **95**, 196401 (2005).
[3] T. D. Krauss, F. W. Wise, and D. B. Tanner, Phys. Rev. Lett. **76**, 1376 (1996).
[4] H. Wu, N. Dai, and P. J. McCann, Phys. Rev. B **66**, 045303 (2002).
[5] P. J. McCann, K. Namjou, and X. M. Fang, Appl. Phys. Lett. **75**, 3608 (1999).
[6] Z. Feit, M. McDonald, R. J. Woods, V. Archambault, and P. Mak, Appl. Phys. Lett. **68**, 738 (1995).
[7] J. R. Ferraro, Appl. Spectrosc. **29**, 418 (1975).
[8] L. Brillson and E. Burstein, Phys. Rev. Lett. **27**, 808 (1971).
[9] T. Shimada, K. L. I. Kobayashi, Y. Katayama, and K. F. Komatsubara, Phys. Rev. Lett. **39**, 143 (1977).
[10] J. G. Shapter, M. H. Brooker, and W. M. Skinner, Int. J. Min. Process. **60**, 199 (2000).
[11] A. Yang, H. Wu, Z. Li, D. Qiu, Y. Chang, J. Li, P. J. McCann, and X. M. Fang, Chin. Phys. Lett. **17**, 606 (2000).
[12] G. D. Smith, S. Firth, R. J. H. Clark, and M. Cardona, J. Appl. Phys. **92**, 4375 (2002).
[13] W. Cochran, R. A. Cowley, G. Dolling, and M. M. Elcombe, Proc. R. Soc. London, Ser. A **293**, 433 (1966).
[14] J. Si, H. Wu, T. Xu, C. Cao, and Z. Huang, Chin. Phys. Lett. **22**, 2353 (2005).
[15] M. Romcevic, N. Romcevic, D. R. Khokhlov, and I. I. Ivanchik, J. Phys.: Condens. Matter **12**, 8737 (2000).
[16] A. I. Belogorokhov, L. I. Belogorokhova, D. R. Khokhlov, and S. V. Lemeshko, Semiconductors **36**, 1063 (2004).
[17] K. Murase and S. Sugal, Solid State Commun. **32**, 89 (1979).
[18] R. W. Grant, J. G. Pasko, J. T. Longo, and A. M. Andrews, J. Vac. Sci. Technol. **13**, 940 (1976).
[19] H. Okumura, H. Ihara, and S. Gonda, J. Vac. Sci. Technol. A **2**, 1329 (1984).
[20] J. I. Pankove, *Optical Processes in Semiconductors* (Prentice-Hall, Englewood Cliffs, NJ, 1971).
[21] H. Burkhard, R. Geick, P. Kastner, and K. H. Unkelbach, Phys. Status Solidi B **63**, 89 (1974).
[22] F. Cerdeira, C. J. Buchenauer, F. H. Pollak, and M. Cardona, Phys. Rev. B **5**, 580 (1972); D. J. Olego, K. Shahzad, J. Petruzzello, and D. Cammack, *ibid.* **36**, 7674 (1987).